

related to the phase transition observed in this temperature range by Menyuk and Dwight.<sup>7</sup>

#### IV. CONCLUSION

We conclude that the bulk of the losses due to  $\text{Fe}^{++}$  ions in ferrites are accounted for by the slow relaxation theory discussed in references 1, 2, and 3. This implies that the magnetic moments of the  $\text{Fe}^{++}$  ions are more tightly coupled to the magnetic lattice than to the crystal lattice at all relevant temperatures. There is, however, some evidence that this theory is an approximation and that the properties of the  $\text{Fe}^{++}$  ions deviate from it to an extent which, while small, is nevertheless observable.

We also conclude that there is more than one ani-

<sup>7</sup> N. Menyuk and K. Dwight, *Phys. Rev.* **112**, 397 (1958).

sotropic loss in the ferrite investigated here, and the simple theory discussed in this work describes each separately, but does not explain why there is more than one. This does not change our conclusion, however, that the bulk of the losses associated with  $\text{Fe}^{++}$  ions are due to a mechanism for which the assumptions given by Eq. (1) are valid.

Finally, an added argument for our conclusion is that the Curie temperatures for the compounds  $\text{FeO}$ ,  $\text{Fe}_2\text{O}_3$ , and  $\text{Fe}_3\text{O}_4$  all lead one to expect exchange frequencies  $\omega_{AB}$  in the compound we have studied which are too large to give  $\omega_{AB}\tau = 1$  for any of the  $\tau$ 's deduced here in the relevant range of temperature.

The authors wish to express their gratitude to J. F. Dillon, Jr., C. Herring, and R. C. LeCraw for critical comments on the manuscript, and S. Geller for an instructive conversation.

### Annealing of Electron-Irradiated GaAs†

L. W. AUKERMAN AND R. D. GRAFT\*  
*Battelle Memorial Institute, Columbus, Ohio*

(Received April 23, 1962)

The annealing behavior of *n*-type GaAs irradiated at room temperature with 1-MeV electrons has been investigated. The fraction *f* of the defects remaining after annealing for a time *t* at an elevated temperature, decays according to the relationship,  $f = a \exp(-\lambda_1 t) + (1-a) \exp(-\lambda_2 t)$ . The rate constants  $\lambda_1$  for various specimens annealed at different temperatures obey the Arrhenius relationship, giving an activation energy of  $1.1 \pm 0.05$  eV.  $\lambda_1$  appears to be an intrinsic property of *n*-type GaAs.  $\lambda_2$ , on the other hand, is dependent on the carrier density, i.e., the annealing is influenced by the position of the Fermi level. The recovery of *p*-type specimens is qualitatively different than that of *n* type. Some preliminary results concerning the effect of irradiation on electrical properties are also included.

#### INTRODUCTION

ANNEALING experiments carried out with irradiated metals have proven to be of considerable value in the interpretation of the type of damage introduced and the kinetics of its recovery.<sup>1,2</sup> Although a number of annealing studies have also been performed with various semiconductors, it does not appear that the details of the recovery of vacancies and interstitials have been completely worked out for any semiconducting material. The recovery of semiconductors may differ considerably from that of metals because of their relatively open lattice structure and different bonding. Furthermore, the position of the Fermi level may have a considerable effect on the annealing behavior of semiconductors.<sup>3-5</sup>

The recovery of compound semiconductors having the zinc-blende structure may be quite different from that of the elemental semiconductors, germanium and silicon. The variety of primordial defects is greater for compounds and the diffusion of a vacancy is, in all cases investigated so far, confined to a given sublattice.<sup>6-8</sup>

This paper is primarily concerned with the recovery of defects produced in GaAs, a semiconductor of the zinc-blende structure, by irradiation at room temperature with electrons of approximately 1-MeV energy. Ideally some irradiations should have been conducted at a much lower temperature, since annealing processes have been observed at temperatures well below room temperature in other semiconductors such as ger-

† This work was supported by the Aeronautical Research Laboratory, U. S. Air Force.

\* Present address: North American Aviation Inc., Columbus, Ohio.

<sup>1</sup> J. W. Corbett, R. B. Smith, and R. M. Walker, *Phys. Rev.* **114**, 1452 (1959).

<sup>2</sup> J. B. Ward and J. W. Kauffman, *Phys. Rev.* **123**, 90 (1961).

<sup>3</sup> J. W. MacKay and E. E. Klontz, *J. Appl. Phys.* **30**, 1269 (1959).

<sup>4</sup> F. H. Eisen, *Phys. Rev.* **123**, 736 (1961).

<sup>5</sup> H. Y. Fan and K. Lark-Horovitz, *Semiconductors and Phosphors* (Interscience Publishers, Inc., New York, 1958), pp. 123-124.

<sup>6</sup> F. H. Eisen and C. E. Birchenall, *Acta Met.* **5**, 265 (1957).

<sup>7</sup> B. Goldstein, *Phys. Rev.* **121**, 1305 (1961).

<sup>8</sup> L. Slifkin and C. T. Tomizuka, *Phys. Rev.* **97**, 836 (1955).

manium,<sup>3,9</sup> silicon,<sup>10</sup> and InSb.<sup>4,11,12</sup> Consequently, in interpreting the present results, one must bear in mind the fact that some of the primordial damage may not have been retained and that some of the radiation-induced defects which are retained might consist of clusters or of complexes composed of vacancies and/or interstitials with various impurities, as has been shown to be the case for silicon<sup>10,13-15</sup> and germanium.<sup>16</sup> Nevertheless, the results of the annealing experiments on all *n*-type specimens studied to date allow a rather straightforward interpretation not necessarily requiring the assumption of complex formation. Eisen's work<sup>4</sup> with InSb also indicates that in this material the radiation-induced defects probably do not interact with impurities.

The present work is concerned exclusively with electron irradiation, since there is little doubt that the damage thus produced is considerably simpler and more readily adaptable to analysis than that produced by irradiation with heavy particles such as deuterons, protons, neutrons, etc. For example, GaAs irradiated with fast neutrons has a component of damage similar to that observed in electron-irradiated specimens as well as a component not produced by electron irradiation that requires a much higher temperature to anneal.<sup>17</sup> It is suspected that this more stable damage is associated with microscopic inhomogeneities produced by the highly energetic atoms which recoil from collisions with fast neutrons. The atoms recoiling from 1-MeV electron bombardment would not have sufficient energy to create many additional displacements. Assuming a threshold displacement energy of about 10 eV,<sup>18</sup> a calculation of the number of secondary displacements produced by 1-MeV electrons indicates that not more than 30% of the primary knock-on atoms possess sufficient energy to create an additional displacement.<sup>19</sup> The resulting picture of the primordial damage is, thus, one of rather closely spaced vacancy-interstitial pairs which are randomly distributed throughout the specimen. As suggested above, some of the initially more closely spaced pairs may not be present at room temperature.

<sup>9</sup> J. W. MacKay, E. E. Klontz, and G. W. Gobeli, *Phys. Rev. Letters* **2**, 146 (1959).

<sup>10</sup> G. D. Watkins, J. W. Corbett, and R. M. Walker, *J. Appl. Phys.* **30**, 1198 (1959).

<sup>11</sup> L. W. Aukerman, *Phys. Rev.* **115**, 1125 (1959).

<sup>12</sup> F. H. Eisen and P. W. Bickel, *Phys. Rev.* **115**, 345 (1959).

<sup>13</sup> G. D. Watkins and J. W. Corbett, *Phys. Rev.* **121**, 1001 (1961).

<sup>14</sup> J. W. Corbett, G. D. Watkins, R. M. Chrenko, and R. S. McDonald, *Phys. Rev.* **121**, 1015 (1961).

<sup>15</sup> G. Bemski, *J. Appl. Phys.* **30**, 1195 (1959).

<sup>16</sup> W. L. Brown, W. M. Augustyniak, and T. R. Waite, *J. Appl. Phys.* **30**, 1258 (1959).

<sup>17</sup> L. W. Aukerman, *Proceedings of the International Conference on Semiconductor Physics, Prague, 1960* (Czechoslovak Academy of Sciences, Prague, 1961), p. 946.

<sup>18</sup> R. Bäuerlein, *Z. Naturforsch.* **14a**, 1069 (1959).

<sup>19</sup> J. Neufeld and W. S. Snyder, *Phys. Rev.* **99**, 1326 (1955).

## EXPERIMENTAL PROCEDURE

### Sample Preparation

"Bridge" type samples were cut from single crystals of GaAs with an ultrasonic tool. The crystals were grown by the gradient freeze technique. The principal impurities in GaAs grown by this method are expected to be silicon, copper, and oxygen.<sup>20</sup> Average sample dimensions were 1×0.2×0.1 cm. It was generally found that measurements were not critically dependent upon surface treatment; etching in a CP-4 solution for a few minutes or lightly sandblasting the surface was sufficient to make all measurements reproducible to within experimental error.

### Electrical Measurements

The electrical properties of interest are the Hall coefficient *R* and the conductivity  $\sigma$ . The carrier density was calculated from the equation

$$R = \pm \gamma / ne, \quad (1)$$

where *n* is the carrier density, *e* is the electronic charge, and  $\pm$  indicates the presence of either positive carriers (holes) or negative carriers (electrons). The factor  $\gamma$  is taken to be unity. This greatly simplifies the calculation of carrier densities and the resulting small errors cannot affect the conclusions. Another quantity of interest is the Hall mobility defined by

$$\mu_H = R\sigma. \quad (2)$$

Current and potential leads were attached to the samples with tungsten pressure contacts after the arms were tinned with indium or plated with rhodium. The samples were mounted in Lavite holders; a thermocouple was attached to the underside of the holder near the sample for temperature measurements. The sample and holder were then placed inside a metal tube (copper or stainless steel) to reduce thermal gradients across the sample. The heater winding was placed on this tube. The entire assembly was sealed in a quartz tube under a helium atmosphere. Hall coefficient and conductivity measurements could be made at temperatures from liquid nitrogen to several hundred degrees centigrade. In making the measurements, the sample current and magnetic field were reversed independently and readings averaged to eliminate thermomagnetic and thermoelectric voltages. All voltage measurements were made with a Leeds and Northrop type K-2 potentiometer.

### Irradiation

The specimens were irradiated at room temperature with approximately 950-keV electrons from a Van de Graaff accelerator.<sup>21</sup> A gentle blast of air was directed

<sup>20</sup> L. R. Weisberg, F. D. Rosi, and P. G. Herkart, *Properties of Elemental and Compound Semiconductors* (Interscience Publishers, Inc., New York, 1960), Vol. 5, p. 25.

<sup>21</sup> The irradiations were carried out with the kind assistance of Dr. Bernard Kulp at the Aeronautical Research Laboratory, Wright-Patterson Air Force Base, Ohio.

TABLE I. Some electrical properties of *n*-type GaAs before and after irradiation.  $n_0$  and  $\mu_0$  are, respectively, the carrier density and mobility before irradiation;  $n_f$  and  $\mu_f$  the carrier density and mobility after irradiation; and  $\phi$  is the integrated electron flux.

Sample designation	$n_0$ ( $10^{16}/\text{cm}^3$ )	$\mu_0$ ( $\text{cm}^2/\text{V}\cdot\text{sec}$ )	$n_f$ ( $10^{16}/\text{cm}^3$ )	$\mu_f$ ( $\text{cm}^2/\text{V}\cdot\text{sec}$ )	$\phi$ ( $10^{16}/\text{cm}^2$ )
246-F	47.5	4970	37.7	4630	20.3
196-2	16.0	4485	12.7	3910	9.3
220-X	11.9	4970	10.0	4630	4.2
184	10.5	4070	8.4	4180	5.4
362-T	9.7	4320	8.4	4180	3.7
144(I)	7.3	2400	4.60	2920	4.0
044(II)	7.3	2360	4.71	1625	14.9
32	3.97	4120	3.20	4210	1.8

against the sample during the irradiation. With this precaution the maximum increase in temperature was approximately 1 deg. All samples were irradiated with the same beam-current setting of  $5.5 \mu\text{A}$ . This value of beam current was determined by collecting the charge which falls upon the sample and the brass-plate sample holder. This method of estimating the dose is not very accurate because of secondary emission from the target and effects of ionization of the air; however, it seems probable that the relative values of flux are fairly reliable.

The specimens were placed 1.2 in. from the port; at this distance the beam was uniform over the entire area of the specimen. Since the range of the electrons is approximately equal to the thickness of the specimens, about 1 mm, the irradiation was carried out for equal times on each side.

### Annealing

Annealing experiments were performed in which samples were alternately cycled between ice temperature and an elevated temperature, called the annealing temperature  $T_A$ . The annealing cycle went as follows: the conductivity was measured with the sample maintained at the reference temperature  $0^\circ\text{C}$ ; the sample was then placed in a high-temperature bath for a measured period of time, then replaced in the ice bath, and the conductivity remeasured. The cycle was repeated until the conductivity had recovered to its pre-irradiation value. From this procedure one can obtain the conductivity as a function of time at the annealing temperature. The degree of recovery is estimated by the fraction not annealed  $f$  defined by

$$f = [\sigma_0 - \sigma(t)] / \Delta\sigma, \quad (3)$$

where  $\sigma_0$  is the conductivity before irradiation,  $\Delta\sigma$  is the change in conductivity due to the irradiation, and  $\sigma(t)$  is the conductivity after annealing a time  $t$ .

To ensure rapid temperature stabilization of the sample, a high heat-capacity bath was designed. The bath consisted of a bismuth-tin eutectic maintained at the annealing temperature by a regulator. A stainless

steel container of silicone oil was immersed in the molten bath; the Lavite holder containing the specimen was dropped into the silicone oil so that the sample was in direct thermal contact with the oil. A copper-constantan thermocouple was placed near the specimen for temperature measurements. After a steady temperature was reached, the bath was capable of maintaining the sample at a constant temperature to within  $0.1^\circ\text{C}$ . The low-temperature bath was a similar container of silicone oil immersed in a slush of ice water.

The finite time required to reach the annealing temperature can be corrected by approximating the smooth rise in temperature by a series of rectangular jumps. Typical heatup times were 2 min, resulting in time corrections of approximately 1 min. The annealing periods were longer than 10 min.

In addition to the isothermal annealing experiments, one *n*-type and one *p*-type sample were annealed isochronally. These experiments were performed primarily to obtain a qualitative picture of the annealing processes. In each case, the specimen was mounted in the holder described under Electrical Measurements. The sample was then rapidly raised to a predetermined temperature for a set period of time (usually about 20 min), cooled to a reference temperature, and the conductivity measured. This cycle was repeated at successively higher temperatures until the conductivity had recovered to its pre-irradiation value.

### EFFECTS ON ELECTRICAL PROPERTIES

The carrier concentration and conductivity of both *n*- and *p*-type GaAs are decreased as a result of electron irradiation. The initial carrier-removal rate of *n*-type specimens having carrier concentrations of about  $10^{17}/\text{cm}^3$  is approximately  $0.45 \text{ cm}^{-1}$ . The effects of the irradiations on the *n*-type specimens which were subsequently annealed are illustrated in Table I. The speci-

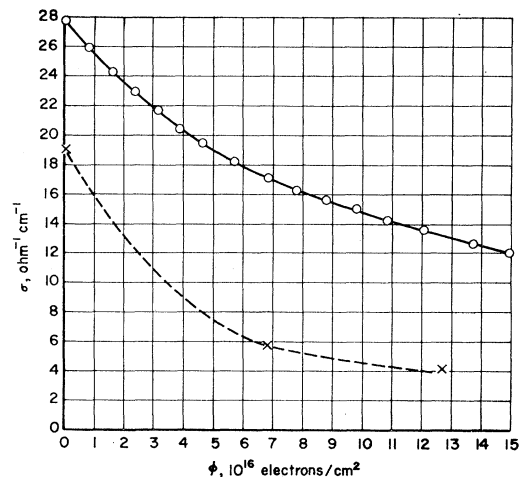


FIG. 1. The conductivity of *n*-type GaAs as a function of integrated electron flux,  $\phi$ . The upper curve is for specimen No. 144 (II) of Table I.

mens numbered 144 (I) and 144 (II) are the same specimen; 144 (I) was irradiated, annealed, and, under the designation 144 (II), re-irradiated.

Irradiation reduces the Hall mobility in most cases; however, several of the lightly irradiated specimens showed an unexpected increase in mobility which appears to be outside experimental error. This increase in mobility is not understood since the introduction of charged scattering centers by the irradiation should result in a decrease in mobility. Although no special attempt was made to investigate this peculiar effect since it is outside the scope of the present study, it is interesting to note that those specimens which increased in mobility were either given a relatively small irradiation or were somewhat more compensated than other specimens. The percentage change in mobility is considerably less than the percentage change in carrier density for all specimens listed in Table I except No. 144 (II). The assumption that the number of defects is proportional to the change in conductivity may still be valid for this specimen, since its annealing behavior was not noticeably different from other specimens.

The temperature dependence of the Hall coefficient indicates that an energy level is introduced by the irradiation at about 0.12 eV or more below the bottom of the conduction band. To avoid perturbing effects due to the variation in the degree of ionization of this level, only specimens whose Fermi levels were at least  $2kT$  above this energy level at  $0^\circ\text{C}$  were selected for annealing studies. With the possible exception of levels lying very near the conduction-band edge (which are difficult to locate by Hall effect measurements) no radiation-induced energy levels lying between the conduction-band edge and the 0.12-eV level mentioned above were detected.

For two specimens the change in conductivity as a function of integrated flux was studied. It is seen in Fig. 1 that the conductivity decreases at a slower rate as the irradiation proceeds. This nonlinearity is not serious as long as the change in conductivity is less than about 35%. All specimens in Table I except 144 (II) were changed less than 35% by their respective irradiations. The upper curve of Fig. 1 is for specimen No. 144 (II).

Possibly the curvature in Fig. 1 is caused by radiation annealing. No room-temperature annealing is observed when the irradiation is stopped. Another explanation, namely, that the curvature results from the presence of an energy level whose probability of occupation is altered as the position of the Fermi level is changed by irradiation, is undesirable for two reasons. First, the level at about 0.12 eV below the conduction band is too far away from the Fermi level of 144 (II) to account for the curvature and no other levels appear to be present which are near the Fermi level; second, the annealing of 144 (II) behaves as if a linear relationship exists between the number of defects and the conductivity of the specimen. It should also be pointed out

that the changes in mobility were not sufficiently large to account for the nonlinearity.

#### ANNEALING EXPERIMENTS

Since the total bombardment-induced change in conductivity  $\Delta\sigma$  was kept rather small (usually 15 to 20% of the initial conductivity), it is assumed that the concentration of defects produced by the irradiation is proportional to  $\Delta\sigma$ . The conductivity always increases and very nearly returns to the pre-irradiation value during annealing. This is the behavior expected if recovery or healing of the radiation damage is taking place.

The results obtained from *n*-type GaAs isochronally annealed for time periods of 15 min are shown in Fig. 2. The specimen was exposed to a total flux of  $9.3 \times 10^{16}$  electrons/cm<sup>2</sup>, reducing the carrier density from 1.6 to  $1.3 \times 10^{17}$ /cm<sup>3</sup>. The values of *f*, the fraction not annealed, are calculated according to Eq. (3). The circles are experimental points, the crosses being explained later. Isothermal annealing experiments discussed below show that the single stage<sup>22</sup> of recovery centered

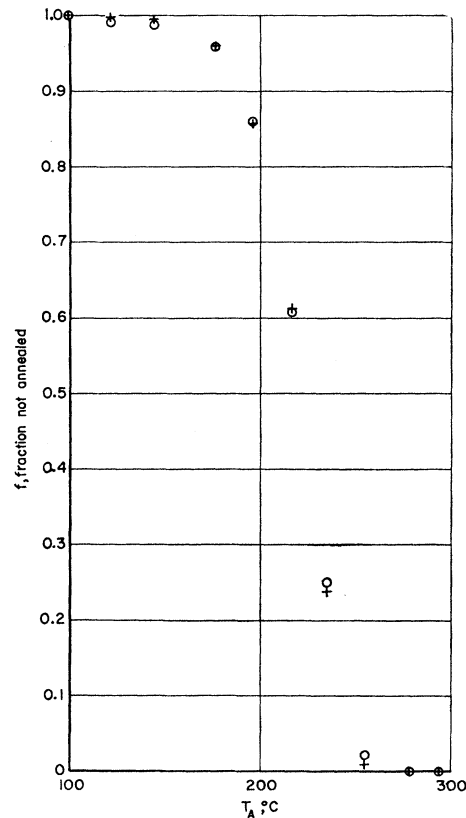


Fig. 2. Isochronal annealing of *n*-type GaAs. The circles are experimental points. The crosses are calculated as discussed in the text. The annealing periods were 15 min at each temperature.

<sup>22</sup> While most samples returned to their pre-irradiation values after the single stage was completed, a few *n*-type samples did not recover completely until temperatures as high as  $400^\circ\text{C}$  were attained. This residual damage was less than 3% in all cases and was sporadic in nature.

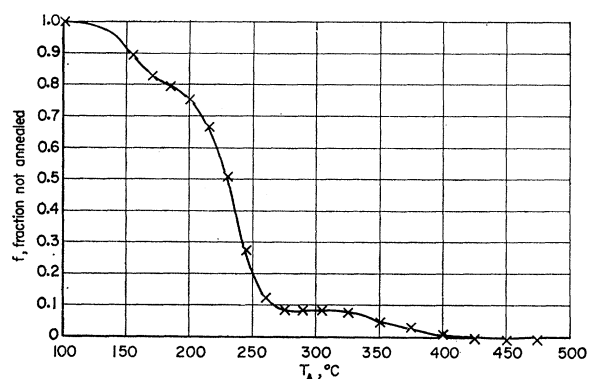


FIG. 3. Isochronal annealing of *p*-type GaAs. The annealing periods were 30 min at each temperature.

near 220°C is composed of two unresolved substages, each obeying first-order kinetics. In Fig. 3 are shown the results of a similar isochronal anneal on *p*-type GaAs. The recovery of *p*-type material is seen to be more complex than *n* type in that two stages are clearly resolved at lower temperatures and a third process is evident at temperatures in excess of 300°C. In contrast to the sporadic high-temperature recovery of *n*-type material, *p*-type GaAs exhibits a well-defined high-temperature recovery stage that accounts for approximately 8% of the total recovery. Detailed isothermal annealing studies were not carried out on *p*-type GaAs.

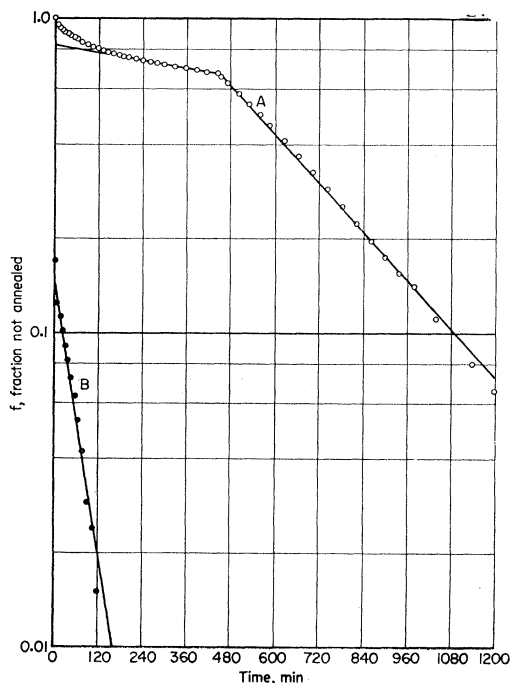


FIG. 4. Isothermal annealing of *n*-type specimen No. 144 (II). During the first branch of curve *A*, annealing time up to 440 min, the annealing temperature was 191.6°C. For times greater than 440 min the annealing temperature was 211.9°C. Curve *B* is the difference between the extrapolated linear portion (solid line of first branch) and the experimental values.

Several specimens of *n*-type GaAs were isothermally annealed at various temperatures. A typical annealing curve is shown as curve *A* in Fig. 4 in which  $\log f$  is plotted as a function of corrected time at the annealing temperature  $T_A$ . By subtracting out the linear portion of curve *A* and replotting the initial points, another straight line curve *B* is obtained. Thus, with the possible exception of a small residual component sometimes present, the entire recovery can be represented by an expression of the form

$$f = a \exp(-\lambda_1 t) + (1-a) \exp(-\lambda_2 t), \quad (4)$$

where  $a$  is a constant and  $\lambda_1$  and  $\lambda_2$  are rate constants. The recovery proceeds as a sum of two independent first-order or monomolecular processes. The same type of behavior was observed for all specimens annealed in this manner.

If the temperature dependence of the rate constants can be expressed as

$$\lambda_i = \lambda_{0i} \exp(-E_i/kT_A), \quad (i=1, 2) \quad (5)$$

where  $\lambda_{0i}$  is a constant and  $E_i$  an activation energy, a plot of  $\log \lambda_i$  vs  $1000/T_A$  for the various specimens should yield a straight line with the slope proportional to the activation energy. Figures 5 and 6 are the curves for  $\lambda_1$  and  $\lambda_2$ , respectively. From Fig. 5 it is seen that the values of  $\lambda_1$  for all specimens lie reasonably close to the straight line representing an activation energy of  $(1.10 \pm 0.05)$  eV. However, in Fig. 6 it is seen that, while the activation energies for each specimen are comparable, the values of  $\lambda_2$  at a given temperature vary over a wide range. (The different points for the same specimen were obtained by changing the temperature of anneal after the  $\lambda_1$  process had reached com-

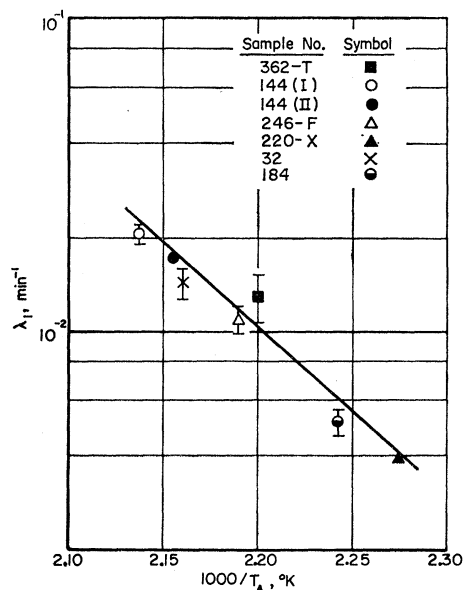


FIG. 5. The values of  $\lambda_1$  for various specimens plotted logarithmically against the reciprocal of the annealing temperature.

pletion as in Fig. 4.) The variations in  $\lambda_2$  from specimen to specimen suggest that this process is conditioned by an extrinsic property of the crystal. The average value of activation energy for the  $\lambda_2$  process is  $E_2=1.60$  eV.

A correlation was found between the values of  $\lambda_2$  and the mean carrier density, which suggested plotting the quantity  $\log(\lambda_2 N_c/\bar{n})$  vs  $1000/T_A$ ,  $N_c$  being the effective density of states in the conduction band and  $\bar{n}$  the mean carrier density over a time interval corresponding to the same temperature of anneal. The plot of  $\log(\lambda_2 N_c/\bar{n})$  vs  $1000/T_A$  is shown<sup>23</sup> in Fig. 7 where the straight line is a least squares fit of all the experimental points and has a slope of 1.55 eV. In Figs. 5 through 7 the estimated uncertainty in determining the points is indicated except in those cases where it is less than about 5%. The relative uncertainty in temperature is estimated to be  $\leq 0.25\%$ . Figure 7 suggests that  $\lambda_2$  is proportional to  $n/N_c$ . A possible interpretation of this result is presented later.

The quantity  $a$  of Eq. (4), which represents the fraction of the damage annealing via the  $\lambda_1$  process, varies from 0.15 to 0.30 from sample to sample. No correlation was found between this quantity and any of the following: carrier density, total irradiation, etch-pit count, or Hall mobility.

In analyzing data like those of Fig. 4, the variation in  $\lambda_2$  resulting from the changes in carrier density as annealing proceeds was not taken into consideration. Although the variation in carrier density during annealing at a given temperature was small for most of these samples, it is not obvious that its effect would be negligible. Therefore, the sample which had undergone the greatest change in conductivity during irradiation [Sample 144 (II)] was analyzed, taking the change in carrier density into account. Considering only the  $\lambda_2$  process, and assuming  $\lambda_2 = \lambda_0 n/N_c$ , we have

$$df_2/dt = -f_2 \lambda_0 n/N_c, \quad (6)$$

where  $f_2$  is now defined analogous to Eq. (3) in terms of the carrier density,

$$f_2 = (n_0 - n)/\Delta n. \quad (7)$$

Eliminating  $n$  from Eqs. (6) and (7) and integrating, one obtains

$$\ln\{f_2/[1 - (\Delta n/n_0)f_2]\} = -\lambda_0(n_0/N_c)t + \text{const.} \quad (8)$$

Thus, the quantity in the curly bracket should be plotted instead of  $f$  in Fig. 4. If this is done for the high-temperature branch, the linearity of the resulting curve is at least as good as the curve shown, and the value of  $\lambda_0$  obtained from the slope of the corrected curve is  $3.66 \times 10^{-2} \text{ min}^{-1}$ , which is to be compared with  $3.53 \times 10^{-2} \text{ min}^{-1}$  for the uncorrected curve. This specimen, for which  $\Delta n/n_0$  was 0.36, requires only a 6% correction.

<sup>23</sup>  $N_c$  and  $\bar{n}$  are determined at the temperature of anneal, assuming an effective mass ratio of 0.06.

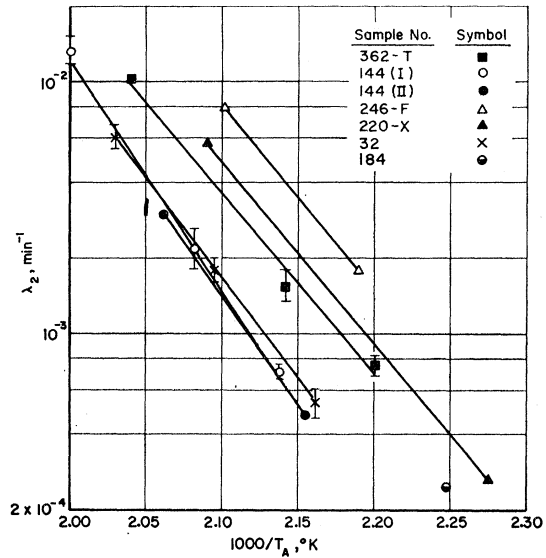


FIG. 6. The values of  $\lambda_2$  for various specimens plotted logarithmically against the reciprocal of the annealing temperature.

For all other specimens,  $\Delta n/n_0$  was considerably smaller than this value.

Using Figs. 5 and 7 to obtain empirical values for  $\lambda_1$  and  $\lambda_2$ , one can predict the experimental values of Fig. 2 fairly well by the use of Eq. (4). Calculated values of  $f$  are shown in Fig. 2 as crosses. The only arbitrarily adjusted parameter was the quantity  $a$ , which was taken to be 0.30 in order to get a good fit. The points near the extremes in annealing temperature

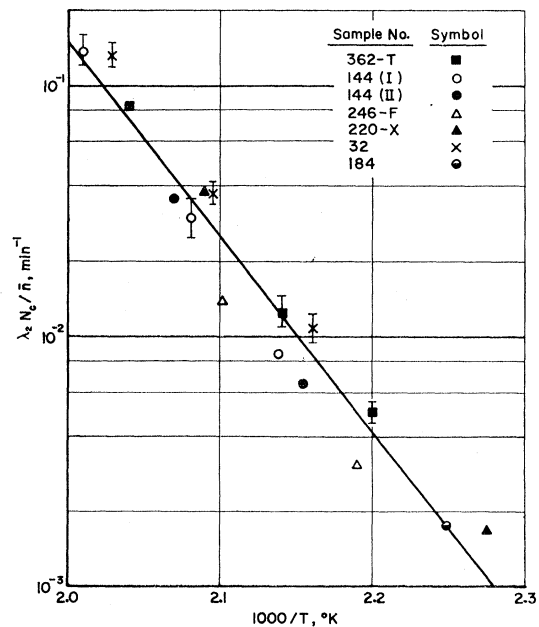


FIG. 7. The same as Fig. 5 except  $\lambda_2$  has been multiplied by the quantity  $N_c/\bar{n}$  which tends to bring the points into better coincidence with a single straight line (see text).

are in rather poor agreement with the data, presumably because of extrapolation errors in obtaining  $\lambda_1$  and  $\lambda_2$  from Figs. 5 and 7. One can see, however, that Eq. (4) gives a good representation of both the isothermal and isochronal experiments.

### DISCUSSION

The most interesting aspect of the annealing behavior of *n*-type GaAs is the correlation of  $\lambda_2$  with carrier density. No other correlations were found. Figure 7 indicates that  $\lambda_2$  at a given temperature is proportional to the carrier density. Since the major impurity is silicon, the question arises as to whether the silicon atoms affect the annealing rate directly, or whether the carrier density or Fermi level is responsible for the variations in  $\lambda_2$ . In view of the rather wide range of compensation present in the specimens (the degree of compensation can be roughly estimated from Hall mobility measurements), it appears that  $\lambda_2$  is not directly dependent on the silicon concentration. To test this hypothesis, a specimen was purposely doped with about  $10^{17}/\text{cm}^3$  tellurium atoms. The silicon content of this specimen, No. 362-T, was estimated to be only  $3 \times 10^{16}/\text{cm}^3$ . It is evident from Fig. 7 that the points for this sample fall in line with other samples; i.e., it is the carrier density and not the silicon concentration which determines  $\lambda_2$ .

The first-order kinetics suggests one of the three following mechanisms: (1) close pair recombination, (2) migration directly to sinks or deep traps, (3) trapping at certain defect sites (such as impurities) followed by migration to sinks. The second mechanism requires the rate constant to be proportional to the concentration of sinks.<sup>24</sup> The third mechanism requires the rate constant to be a function of both sink concentration and trap concentration.<sup>25</sup> If either of these mechanisms were operating, the sink concentration for the  $\lambda_1$  process would be constant from sample to sample, within about 10 to 20%, and the sink concentration for the  $\lambda_2$  process would be proportional to the carrier density to within about 30 or 40% (assuming the processes involved are independent of the position of the Fermi level). If the sinks are accidental impurities or dislocations, their concentration is expected to vary widely from sample to sample, in which case the closeness of the experimental points to the straight lines in Figs. 5 and 7 would be highly fortuitous.

Indeed, since dislocations are naturally suspected of being good sinks for vacancies or interstitials, etch-pits counts<sup>26</sup> were made on a (111) face of two of the specimens irradiated. For specimen Nos. 32 and 362-T, the counts were  $6 \times 10^3/\text{cm}^2$  and  $10^5/\text{cm}^2$ , respectively. Another specimen, cut from the same ingot as sample No. 144, showed about  $10^6$  etch pits/ $\text{cm}^2$ . This large

variation in etch-pit counts suggests that dislocations are not playing a major role in the annealing. In view of the large dislocation densities, migration to surfaces seems rather unlikely. Thus, it appears that, of the annealing mechanisms considered, direct recombination of close pairs is the most plausible.

The dependence of  $\lambda_2$  on carrier density is consistent with the following hypothesis: Associated with the defect responsible for the  $\lambda_2$  process is an electronic state which when occupied lowers the barrier for migration or recombination, as the case may be. The following treatment based on this hypothesis does not require a detailed knowledge of the annealing mechanism involved. There may be a number of conceivable mechanisms in which a thermally activated process is influenced by the occupation of an electronic state. For example, the occupation of the electronic state may increase the Coulomb attraction between members of close vacancy-interstitial pairs. This is similar to the mechanism which has been suggested<sup>4</sup> to account for part of the annealing of InSb. It is also interesting to consider the possibility that the postulated electronic state is associated with a bonding or antibonding orbital localized at the interstitial or vacancy. For example, an antibonding orbital at a vacancy would, when occupied, cause a relaxation of some of the forces pulling nearest neighbor atoms together. This might enable a next-nearest neighbor or a nearby interstitial to jump into the vacancy. Watkins and Corbett<sup>3</sup> have suggested the use of antibonding orbitals to account for some of the spin-resonance phenomena observed in electron-irradiated silicon. The present work, however, leaves such questions concerning the detailed nature of the defects and associated electronic states unanswered.

On the basis of the above hypothesis, the observed dependence of annealing on carrier density (or Fermi energy) can be easily derived. The fraction of the defects in which the postulated electronic state is occupied is

$$\psi = N^*/N = \{1 + \exp[(\epsilon - \zeta)/kT]\}^{-1}, \quad (9)$$

where  $\zeta$  is the Fermi energy,  $\epsilon$  is the energy level associated with the electronic state as measured from the bottom of the conduction band,  $N^*$  is the concentration of occupied defects, and  $N$  is the total concentration of defects. Assuming that only the occupied defects  $N^*$  are mobile, we have

$$dN/dt = dN^*/dt = -\lambda N^* = -\lambda \psi N. \quad (10)$$

This, of course, assumes a first-order process with  $\lambda$  as the rate constant. Thus, the experimental rate constant  $\lambda_2$  is to be identified with  $\lambda \psi$ . If  $\epsilon$  lies near the bottom of the conduction band or above it, the following approximation for Eq. (9) is quite accurate:

$$\psi \cong \exp[(\zeta - \epsilon)/kT], \quad (11)$$

<sup>24</sup> R. C. Fletcher and W. L. Brown, Phys. Rev. **92**, 585 (1953).

<sup>25</sup> A. C. Damask and G. J. Dienes, Phys. Rev. **120**, 99 (1960).

<sup>26</sup> J. L. Richards and A. J. Crocker, J. Appl. Phys. **31**, 611 (1960).

since for the specimens under consideration  $\zeta$  is considerably below the bottom of the conduction band at the annealing temperature. Utilizing the Arrhenius expression,

$$\lambda \propto \exp(-E/kT), \quad (12)$$

we have

$$\lambda_2 = \lambda \psi \propto \exp[-(E + \epsilon - \zeta)/kT]. \quad (13)$$

Since classical statistics are valid for the specimens at the annealing temperatures under consideration, we have

$$\exp(\zeta/kT) = n/N_c, \quad (14)$$

giving

$$\lambda_2 N_c / n \propto \exp[-(E + \epsilon)/kT]. \quad (15)$$

Thus, the apparent activation energy as measured from the slope of the straight line in Fig. 7 is  $E + \epsilon$ , where  $E$  represents the barrier which a defect must overcome in jumping from one position to another and  $\epsilon$  is related to the probability that the electronic state mentioned above is occupied.

Whether or not the defects recovering by the  $\lambda_2$  process are vacancy-interstitial pairs or trapped defects is an open question; however, the authors believe the vacancy-interstitial pair hypothesis is the more plausible. If the trapped-defect hypothesis were correct, the above mathematical model would still apply, but the concentration of sinks would have to be constant within about 30 to 40% from sample to sample.

The interpretation of the isochronal annealing of the  $p$ -type sample, Fig. 3, remains uncertain. One is tempted to identify the first jog in Fig. 3 with the  $\lambda_1$  process in  $n$ -type samples, and the second jog with the  $\lambda_2$  process. But if this is done, a certain amount of caution is necessary, especially in the latter case. For, if the above model of the  $\lambda_2$  process is correct, the rate constant would be decreased by approximately  $e^{E_G/kT}$  for  $p$ -type samples, where  $E_G$  is the band gap, about 1.4 eV for GaAs. Such small rate constants could not account for the annealing in Fig. 3. Therefore, if the second jog in Fig. 3 is assumed to involve the disappearance of the same defects as the  $\lambda_2$  process in  $n$ -type GaAs, one must postulate a different annealing mechanism for  $p$ -type samples. The second jog of Fig. 3 can be fitted to a first-order process with an activation energy of  $1.3 \pm 0.3$  eV. The corresponding rate constant at a given temperature is about an order of magnitude

lower than the average  $\lambda_2$  value for  $n$ -type samples at the same temperature.

The third jog in Fig. 3, the one occurring at about 350°C, possibly represents the annealing of deep-lying donors which, being un-ionized, would have no effect on the carrier density of  $n$ -type samples and only a very small effect on their mobility. This idea is consistent with the fact that sample No. 144, after the first irradiation and annealing cycle (Table I), showed no net change in carrier density but a slight decrease in mobility.

#### SUMMARY

The annealing of  $n$ -type GaAs irradiated with electrons at room temperature can be described in terms of two independent first-order processes as in Eq. (4). The rate constant for the first process can be fitted to an Arrhenius plot (Fig. 5) in spite of rather wide variations from sample to sample in impurity concentration, carrier concentration, dislocation density, etc. The slope of such a plot gives an activation energy of  $(1.10 \pm 0.05)$  eV. The Arrhenius plot of the rate constant for the second process shows much greater scatter (Fig. 6); however, the scatter is significantly decreased if the rate constant is multiplied by  $N_c/\bar{n}$ , where  $N_c$  is the effective density of states and  $\bar{n}$  the average carrier density during annealing at a given temperature (Fig. 7). This behavior can be explained if it is assumed that the diffusion of the annealing defect is dependent upon the occupation of an electronic state which has a very low probability of occupation. If this interpretation is correct, the apparent activation energy  $(1.55 \pm 0.05)$  eV is made up of two components: one which relates to the occupation probability of the electronic state and one which relates to the jumping probability of the defect.

Comparison of  $p$ -type and  $n$ -type specimens indicates important differences in annealing behavior; however, the former were not studied in detail.

#### ACKNOWLEDGMENTS

The authors wish to acknowledge the Compound Semiconductor Research Group of Battelle Memorial Institute for the samples of GaAs. Helpful suggestions from Dr. E. M. Baroody and Dr. A. C. Beer were greatly appreciated. The assistance and cooperation of Dr. Bernard Kulp made these experiments possible.